ЖЭТФ, 1998, том 113, вып. 3, стр. 805–815

GAIN OF A COMPRESSED DT FUEL STATISTICALLY IGNITED BY A MULTISPARK ASSEMBLY

A. Caruso, C. Strangio

Associazione Euratom — ENEA, CRE Frascati
00044, Frascati (Roma), Italia

Submitted 10 June 1997

Most of the current inertial confinemet fusion (ICF) schemes are based on the ignition of a high-density DT fuel by a single, high-temperature spherical hot spot (the spark). The spark is self-generated by the implosion process, which is used to bring the fuel to high density. To start ignition the spark has to be dimensioned in such a way that the ion temperature would be greater than 5–7 keV, and that the spark radius would be greater than the α-particle range. A spark with these features is indicated as supercritical. In the scheme based on self-generated spark, ignition can fail to occur when the produced spark strongly deviates from spherical shape, which can make all the surface losses highly relevant. High deformation, or even spark splitting, can occur due to the amplification of initial deviations from spherical shape by hydrodynamic instabilities (or by secular growth) during the implosion process. In principle, ignition can be recovered if the implosion is designed in such a way as to make supercritical at least one of the portions of hot fuel which are produced in this way near stagnation. As a general trend, more compressed final assemblies are required. In this paper we present fuel gain calculations (Gain = Thermonuclear energy/Energy in the compressed fuel) for DT assemblies ignited at the end of an implosion process by a supercritical spark statistically created within a cluster of many subcritical ones. It is assigned the total number of sparks and the probability of having at least one of them supercritical. As a function of these quantities we calculate, in the framework of an isobaric model, the average thermal energy associated with the spark assembly. The same model is also used to evaluate, by statistical arguments, the areal mass, the burn fraction, and the system's total fuel gain. It is found that the energy distribution function of the sparks is influenced only by a single global parameter, in which the assigned ignition probability and the number of sparks are also represented. Compared to the single central-spark approach, being the final states with allowed inner turbulence, the multispark scheme is characterized by relaxed initial symmetry requirements. For multispark systems we can realistically consider the achievement of fuel gains comparable or greater than those typical of the single-spark approach, when evaluated for currently accepted spark convergence ratios. With regard to the single spark case, higher cold fuel densities are needed, as expected (typically 2×–3×, for the same gain, depending on the energy distribution function).

1. INTRODUCTION

The conventional ICF scheme is based on fuel triggering by a single, self-generated hot spot (the ignition spark) at the center of a compressed, cold DT fuel assembly. Hot spot ignition is usually preferred to volume ignition because, in the cases of interest for the energetic application of ICF, it provides higher fuel gains at substantially smaller extreme parameters for the compressed fuel assembly (pressure, density, density × fuel size). This is basically due to the circumstance that, to get high fuel gains in uniform systems it is necessary to ignite the fuel at comparatively low temperatures. This requires radiation trapping, in order to make radiative losses smaller than the thermonuclear energy released to the fuel.

In the central spark approach, ignition is initiated when the ion temperature in the spark, T_i ($\approx T_e$, the electron temperature), is greater than 5–7 keV and the spark radius, R_{spark}, is greater than the range of the α-particle produced in the DT reaction. Under such conditions, in a stagnant spark the thermonuclear energy deposited inside the spark exceeds the radiative and the electronic conductivity losses, and self-heating occurs. A spark with these features is called as supercritical spark.

Burn propagates from the spark to the surrounding fuel, bringing it to temperatures in the range of 40–100 keV. Fuel combustion is quenched by hydrodynamic expansion in a time $t_{exp} \approx R_{fuel}/4c_s$, where R_{fuel} is the total radius of the compressed fuel and c_s is the sound velocity at the burning temperature (much greater than the ignition temperature). The governing number for this process is clearly $\phi = \langle\sigma\nu\rangle_{\rm DT}(\rho/M_{\rm DT})t_{exp}$, where $\langle\sigma\nu\rangle_{\rm DT}$ is the usual Maxwellian averaged product of the DT reaction cross section times the ion velocity, ρ is the fuel mass density, and $M_{\rm DT}$ is the ionic average mass. The maximum of ϕ occurs at a temperature $T \approx 40.6$ keV and is $\phi_{max} \approx \rho R_{fuel}/4.7$ (CGS units are used). It is therefore clear that values of ρR_{fuel} of several g/cm^2 are needed to obtain high values for the fractional fuel burn, f_{burn}. A widely used formula for f_{burn} is given in the next section. Typically, for $\rho_{fuel} = 0.3$, we have $f_{fuel} = 0.3$. The value R_{spark} of the spark radius is typically assumed to be of the order of 1/40 of the initial fuel capsule radius R_{target} of the (i. e. the convergence ratio is $C_{spark} = R_{target}/R_{spark} = 40$). Such a large value of C_{spark} is used to maintain the ablation pressure, needed to drive the fuel up to the required high implosion velocity, within technically available values (at laboratory energy releases).

The controlled formation of the ignition spark is a main issue in this scheme. Actually, due to the required high convergence ratio, this target design seems sensitive to nonuniformities in the ablation pressure, to irregularities in the target structure, and to hydrodynamic instabilities. For instance, it has been shown [1], how due to the nonuniformities in the initial energy deposition (percent sized low modes, mode number l up 10–20), the thermonuclear gain can drop abruptly to zero. The reason for ignition failure (no gain) is the formation of a highly deformed spark, in which the surface heat losses, due to an unfavourable surface-to-volume ratio, are too large. Numerical modeling shows that because of hydrodynamic instabilities, the final spark, at stagnation, can be so distorted as to become nearly split into l substructures by the well-known mushroom-shaped jets [2, 3]. Preliminary studies [3] of $3D$ perturbed spherical stagnation show that saturation occurs when the perturbation amplitude is of the same order of wavelength. These studies have been made for the single mode at low harmonic indices (l and m up 6).

It should be noted that low modes (mode indices 5–10) can, in principle, generate a large number of substructures. If the prevailing grain size is of the order of R_s/n (R_s is the radius within which the sparks are enclosed, and n is a typical mode number), approximately n^2 fragments saturated at R_s/n can be allocated on a single spherical layer, while n^3 can be allocated in a volume. At any rate, unbalanced direct irradiation with multibeam modern laser installations may already produce a large number of substructures ($n \propto$ (number of beams)$^{1/2}$).

To the best of our knowledge, multimode $3D$ studies with realistic implosion dynamics and burn are still lacking, as is any acceptable theoretical description for the final turbulence, as it may result for given initial conditions. However, for conventional target designs, it seems reasonable to assume that, unless very high spherical symmetry is achieved in the initial stages of the implosion (by high-quality irradiation and target finish), spark splitting and ignition failure at stagnation can occur.

Let us assume that the initial requirements for symmetry are deliberately relaxed, so that

a final turbulent condition is allowed. In this context, an interesting question which must be be answered has to do with the possibility of recovering ignition and high gain for this final assembly. Clearly, to find the answer, the relevant key parameter to be determined is the investment in energy required to make supercritical, with assigned probability p, at least one of the hot fuel portions in the turbulent mix (in the center or elsewhere). Once this energy is determined, the assembly parameters needed for high gain can be also found. This information can then be used to identify the general features of implosions which may lead to such final configurations. Since an ignition probability p is introduced, the question may arise about the scheme's usefulness for energy applications, as now a finite ignition failure probability $(1-p)$ is allowed. In energy applications, however, the concept of ignition failure can be introduced without harm, if the implosion is designed in such way as to make the ignition probability p sufficiently high. For this kind of design, the well-known reactor loop condition, which relates the target gain to the driver efficiency η_{driver}, say $\eta_{driver} \times$ target gain ≈ 10, needs only be changed to $p \times \eta_{driver} \times$ target gain ≈ 10. Ignition failure can arise under reactor conditions for a number of reasons, different from target design (e.g., misalignment, target structural imperfections, lack of reproducibility of the driver pulse, etc.), so that the probability of ignition p should to be introduced in any case.

2. A MODEL FOR GAIN CALCULATIONS

The following model is adopted to answer the questions discussed in the previous section.

a) Uniform pressure (P) is assumed at stagnation for the final fuel assembly. Ignition and fuel gain calculations with this assumption have been made by a number authors [4] since 1976.

b) The fuel is divided into two phases, hot and cold. The hot fuel is assumed to be split into N parts at the same temperature. Having the same temperature and pressure, the hot sparks have also the same density (ρ_{spark}). The pressure in the cold fuel is assumed to be

$$P = \alpha P_F, \tag{1}$$

where α is the factor by which this part of the fuel is not degenerate, and P_F is the Fermi pressure [5].

c) The compressed DT fuel assembly is assumed to be a perfect gas. Thus the energy per unit volume is $3P/2$ everywhere, regardless of the degeneracy degree [6].

d) Lacking better descriptions, simple test-distribution-functions for the turbulence spectrum in energy are adopted (size $\propto$ energy$^{1/3}$). Various dependences are tried for trend sampling. The final gain is computed for the distribution which gives the smaller gains in the explored set.

e) To ignite the assembly, we assume [5] there must be at least a spark with energy (E) such that

$$E > E_{thr} \approx \frac{91}{\rho_{spark}^2} \frac{T_{spark}}{7} \text{ MJ}, \tag{2}$$

where T_{spark} is in keV, and ρ_{spark} is in g/cm^3. The inequality (2) holds for a set of spheres with a radius $R \geq 0.3/\rho_{spark}$ cm and the same density (ρ_{spark}) and temperature (T_{spark}). To obtain ignition a $T_{spark} = 5$ keV is usually considered sufficient. In all the following numerical examples $T_{spark} = 7$ keV will be assumed. Unless a critical spark ($E > E_{thr}$) has been created

in the assembly, the subcritical sparks ($E < E_{thr}$) are ultimately cooled by thermal conduction, radiative losses or the general assembly expansion.

f) The probability p to have within N sparks at least one with $E \geq E_{thr}$ is assigned. Once p and the energy distribution function for sparks are assigned, the total spark energy (E_{hot}) can be calculated in terms of E_{thr}, N, and p.

g) The gain calculations require an estimate for the fraction (f_{burn}) of mass burned by thermonuclear reactions before the general fuel disassembling occurs. For DT fuel assemblies with spherical symmetry we apply a widely used formula [5] for f_{burn}

$$f_{burn} = \frac{\int_0^{R_{fuel}} \rho\, dr}{\int_0^{R_{fuel}} \rho\, dr + 7} \text{ [CGS units]}, \tag{3}$$

where the integral is taken from the symmetry center to the radius of the total fuel assembly R_{fuel}. In our case we use a variant of Eq. (3), in which the integral is statistically evaluated.

3. THE PROBABILITY OF IGNITION

We assume that, as a result of the implosion, within the isobaric fuel N hot sparks have been formed and distributed in energy E according to $dq = f(E, E_0)dE$, where E_0 is a parameter with dimensions of energy and dq is the probability for a spark to be between E and $E + dE$. Let $f(E, E_0) = \omega(E/E_0)/E_0$, where ω is a dimensionless function. The probability p to have at least one supercritical spark can easily be calculated in terms of ω as

$$p = 1 - \left[\int_0^{E_{thr}/E_0} \omega(x)dx \right]^N . \tag{4}$$

This equation can be solved for E_0 as a function of E_{thr}, p, and N. After this value of E_0 is inserted in

$$E_{hot} = N \int_0^\infty E f(E, E_0)dE = N E_0 \int_0^\infty x\omega(x)dx, \tag{5}$$

an estimate results for the total energy, E_{hot}, which is required in order to obtain, with assigned probability, at least one above-threshold spark. Clearly,

$$E_{hot} = \gamma E_{thr}, \quad \gamma = Nh\left[(1-p)^{1/N}\right], \tag{6}$$

where the function h is calculated from Eqs. (4) and (5). We note that, when N is large, the expected p-dependence for γ can be slow.

Since $E \propto R^3$, where R is the radius of the spark, to use ω is tantamount to using the space turbulence spectrum. The distribution functions in E can then be seen in terms of spark

radii by introducing a space scale R_0 through $E = (R/R_0)^3 E_0$, so that the function $f(E, E_0)$ will correspond the function

$$g(R, R_0) = R_0 f(E, E_0) \frac{dE}{dR}. \tag{7}$$

We now consider a few examples of the distribution functions in E, chosen to illustrate some relevant points in view of their mathematical simplicity. We adopt three functions, a square-box, an exponential, and a simple combination of power-laws in energy, which qualitatively represent quite different energy (radii) distributions. The square-box dependence is

$$f(E, E_0) = \frac{1}{E_0} \quad \text{for} \quad E \leq E_0, \tag{8}$$

$$f(E, E_0) = 0 \quad \text{for} \quad E > E_0, \tag{9}$$

and the corresponding normalized energy is

$$\gamma = \frac{N}{2(1-p)^{1/N}}. \tag{10}$$

The exponential dependence

$$f(E, E_0) = \frac{\exp(-E/E_0)}{E_0} \tag{11}$$

corresponds to

$$\gamma = -\frac{N}{\ln\left[1-(1-p)^{1/N}\right]}, \tag{12}$$

and for the power-laws case

$$f(E, E_0) = \frac{2}{3}\left[1 - \left(\frac{E}{E_0}\right)^{1/3}\right]\left(\frac{E}{E_0}\right)^{-2/3}\frac{1}{E_0} \quad \text{for} \quad E \leq E_0,$$
$$f(E, E_0) = 0 \quad \text{for} \quad E > E_0, \tag{13}$$

$$\gamma = \frac{N}{10\left[1-\sqrt{1-(1-p)^{1/N}}\right]^3}. \tag{14}$$

The dimensionless hot energy γ (in units of N) is represented as a function of p in Fig. 1, for $N = 10$. It is worth noting how already for this value of N both the «exponential» and the «power-laws» functions give better results than the «square-box» function. As is obvious from Eqs. (10), (12), and (14), the dependence on p becomes less important for increasing N. Note also that E_{hot} is substantially smaller than NE_{thr}.

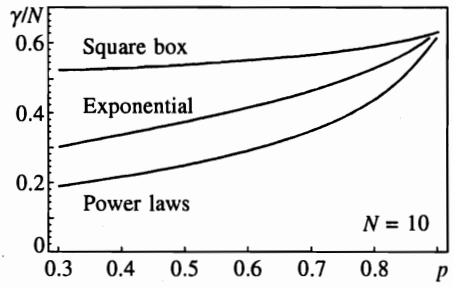

Fig. 1. Dependence of the parameter γ/N on p. The calculations are presented for the distribution functions given by Eqs. (8), (9), (11), and (13)

4. FUEL ASSEMBLY DIMENSIONS

Let us assume that an energy E_{fuel} has been transferred to the compressed fuel. The fraction

$$\nu = E_{hot}/E_{fuel} \tag{15}$$

is used to parametrize our calculations. If the parameter ν is given, by using Eq. (6), we can write the allowed E_{thr} as follows:

$$E_{thr} = \frac{\nu}{\gamma} E_{fuel}, \tag{16}$$

so that the allowed hot fuel density, ρ_{spark}, can be computed from Eq. (2). Since the temperature is given (say, $T_{spark} = 7$ keV), we can find the hot fuel pressure. Because the system is isobaric, the pressure (P) is the same everywhere in the fuel. Equation (1) can then be used to determine the cold fuel density, ρ_{cold}. The energy density throughout the fuel is $3P/2$, so that when we assume the fluid is entirely enclosed within a sphere of radius R_{fuel} (see Fig. 2), the system size is

$$R_{fuel} = \left(\frac{E_{fuel}}{2\pi P}\right)^{1/3}. \tag{17}$$

Similar considerations provide the total fuel mass, as a sum of the cold and hot part contributions:

$$M_{fuel} = \frac{2}{3}\left[\rho_{cold}(1-\nu) + \rho_{spark}\nu\right]\frac{E_{fuel}}{P}. \tag{18}$$

Since the critical spark volume is $E_{thr}/(3P/2)$, from the previous formulas the critical spark radius is found to be

$$R_{thr} = (\nu/\gamma)^{1/3} R_{fuel}. \tag{19}$$

We note that the distribution function in energy (or R) enters in these estimates only through the single dimensionless parameter γ introduced in the initial E_{thr} evaluation [through Eq. (16)].

The thermonuclear gain for this fuel assembly is then

$$G = \varepsilon_{tn}\frac{M_{fuel}}{E_{fuel}} f_{burn}, \tag{20}$$

where ε_{tn} is the thermonuclear energy released by burning the unit mass, and f_{burn} is the fraction of burned mass, now to be evaluated by a statistical version of Eq. (3).

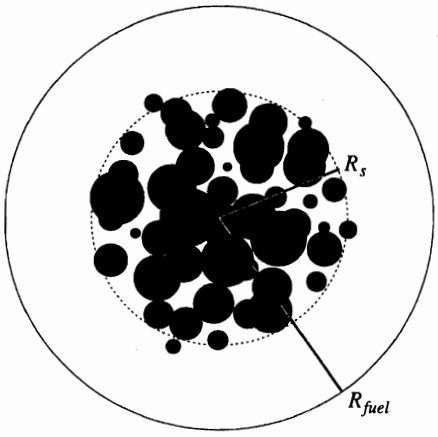

Fig. 2. The numerical examples reported in the paper refer to sparks randomly distributed within a sphere of radius R_s smaller or equal to the fuel radius R_{fuel}

5. THE BURN FRACTION f_{burn}

For the situation analyzed in this paper, the integral appearing in the Eq. (3) for f_{burn} is

$$\int_0^{R_{fuel}} \rho\, dr = \rho_{spark} L_{spark} + \rho_{cold}(R_{fuel} - L_{spark}), \tag{21}$$

where L_{spark} is obtained by adding the portions of the radius R_{fuel} embedded in the randomly distributed sparks (e.g., the dashed segments in Fig. 2).

Let us assume that a line starting from the system's center meets a spherical spark of radius R ($\propto E^{1/3}$). It is easily seen that, on the average, the line segment within the sphere is $(4/3)R(E)$. If, along the radial coordinate r in the fuel, the space-energy distribution is then assumed to be $dN = 4\pi r^2 n(r) f(E, E_0) dr\, dE$, we obtain

$$L_{spark} = \int_0^{R_{fuel}} dr \int_0^{\infty} dE\, n(r) f(E, E_0) \pi R^2(E) \cdot \frac{4}{3} R(E). \tag{22}$$

However, $(4/3)\pi R^3 = 2E/(3P)$, where P is the constant presure of the system, so that through Eqs. (5), (17), and (19) follows that

$$L_{spark} = R_{fuel} \nu \left(\frac{R_{fuel}}{R_{turb}} \right)^2, \quad R_{turb}^2 = N \left[\frac{4\pi}{3} \int_0^{R_{fuel}} n(r) dr \right]^{-1}, \tag{23}$$

without any additional assumption on the distribution function $f(E, E_0)$. As we have seen in the previous section, the system dimensioning depends on $f(E, E_0)$ only through γ. Thus the entire model depends only on the integral parameters γ and R_{turb}.

If the sparks are distributed uniformly in the volume enclosed within a radius $R_s \leq R_{fuel}$ (see Fig. 2), through Eq. (23) we find $R_{turb} = R_s$ and

$$L_{spark} = R_{fuel} \nu (R_{fuel}/R_s)^2. \tag{24}$$

For this case, a more convenient parameter, the dilution of the sparks (d), can be used instead of R_s:

$$d = \frac{4\pi R_s^3}{3}\left(\frac{2E}{3P}\right)^{-1} = \frac{1}{\nu}\left(\frac{R_s}{R_{fuel}}\right)^3, \tag{25}$$

where Eqs. (15) and (17) were used. By definition $d \geq 1$. After d is assigned in the parametrization, we require $\nu d = (R_s/R_{fuel})^3 \leq 1$, so that $\nu \leq 1/d$. In terms of d, $L_{spark} = R_{fuel}(\nu/d^2)^{1/3}$, so that finally

$$\int_0^{R_{fuel}} \rho\, dr = \left[\rho_{cold} - (\rho_{cold} - \rho_{spark})\left(\frac{\nu}{d^2}\right)^{1/3}\right] R_{fuel}. \tag{26}$$

Since $\rho_{cold} > \rho_{spark}$, the integral (and f_{burn}) increases with d.

The conventional calculations for single, central spark [5] can be formally recovered from this model by setting $\gamma = 1$ and $d = 1$. From Eqs. (15), (16), (19), (24), and (25) it results in $E_{hot} = E_{thr}$, $L_{spark} = R_s = R_{thr}$, and the statement holds.

6. FUEL GAIN CALCULATIONS

In the following we present some gain evaluations for assemblies having the sparks dispersed uniformly within a radius $R_s \leq R_{fuel}$ [see Fig. 2, and Eqs. (24)–(26)]. The uniform distribution in the entire fuel is obviously included as a special case ($\nu = 1/d$). The relevant formula for f_{burn} is that obtained by using Eqs. (3) and (26).

The numerical results presented in this section refer to $E_{fuel} = 400$ kJ; this value is taken just for illustrative purposes. Here, we are not interested in the value of the gain which can be achieved, but in its relative change as a function of the number of sparks N. In all the calculations, the ignition temperature was assumed to be 7 keV (see Eq. (2)).

All the graphs presented refer to an ignition probability $p = 0.9$ (unless the lowest values of N are considered, the results are largely insensitive to the value of this parameter (see Fig. 1). The ratio between the fuel pressure and the Fermi pressure, in the cold fuel, was assumed to be [8] $\alpha = 2$. The typical behavior of the gain G in terms of ν and d is illustrated in Fig. 3, where the isolevels for G are shown. The behavior is always qualitatively the same, regardless of which values of N and p are considered, or the distribution function in energy is adopted.

The curve *1* represents the boundary for the region where $\nu \leq 1/d$ ($R_s \leq R_{fuel}$; see Sec. 5). The points on *1* represent uniform distributions of the sparks throughout the fuel volume ($R_s = R_{fuel}$). The curve *2* represents the loci where a maximum of G occurs for assigned d. On this curve, in the region below the point A, $(\partial G/\partial \nu)_d = 0$. An additional modest increase in G can be obtained by moving along the curve *1* from A to the point B, where the line *1* is tangent to an isolevel [on this path $(\partial G/\partial \nu)_d \geq 0$]. The gain evaluated in B is the highest possible. The coordinates of B are given in Table for the «square-box» distribution function (and $p = 0.9$). Lying on the curve *1*, these B points correspond to a uniform spark distribution in the fuel (i. e., $R_s = R_{fuel}$).

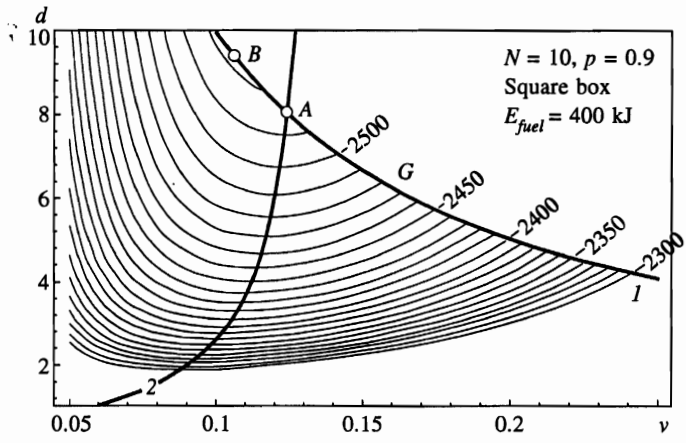

Fig. 3. Gain isolevels in the ν, d plane. The parameter $\nu = E_{hot}/E_{fuel}$ represents the total energy given to the sparks, measured in units of the total fuel energy E_{fuel}. The dilution parameter d represents the ratio of the volume in which the sparks are distributed (radius R_s) to the overall sparks volume. Between the curve *1* and the line $d = 1$ lie the physically interesting points, those for which $R_s \leq R_{fuel}$. On the curve *2* lie the points of maximum gain at assigned d. The maximum possible gain is achieved on B, where *1* is tangent to an isolevel

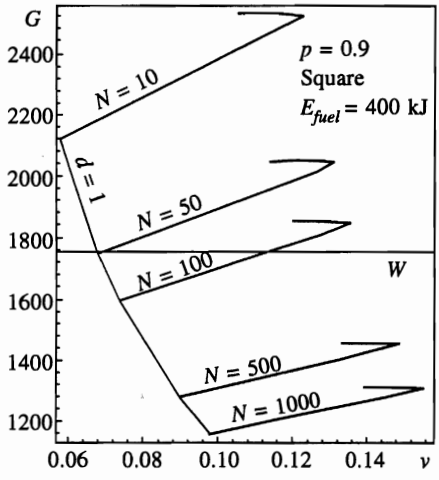

Fig. 4. The maximum gain (evaluated along the line *2* in Fig. 3, and then from A to B) is reported for different values of N. The starting value is $d = 1$.

N	ν	d	G
10	0.1061	9.423	2523
50	0.1148	8.710	2042
100	0.1197	8.353	1845
500	0.1329	7.526	1445
1000	0.1394	7.174	1297

The maxima corresponding to different values of N are shown in Fig. 4 for the «square-box»

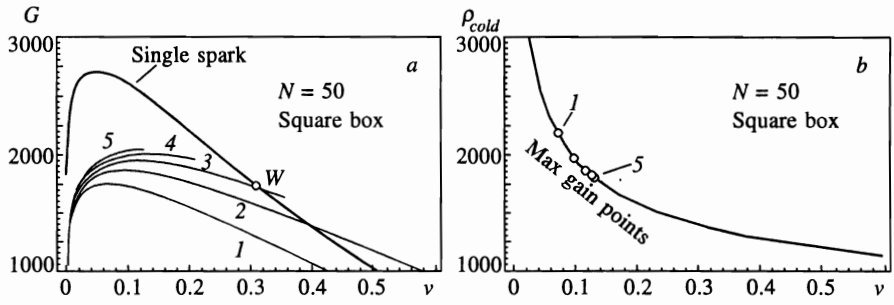

Fig. 5. *a*) Fuel gain for the case of 50 sparks distributed in energy according to the «square-box» distribution; $p = 0.9$, $E_{fuel} = 400$ kJ; *1* — $d = 1$, *2* — $d = 1.7$, *3* — $d = 2.8$, *4* — $d = 4.8$, *5* — $d = 8$. *b*) Cold fuel density plotted as a function of ν

distribution (following curve *2* up to the point A, and then the curve *1* from A to B). Along each curve the value of the parameter d changes from 1 to the corresponding B points, which are listed in Table. The sudden change in direction of each curve occurs at the transit through the A points (see Fig. 3). In Figs. 5*a* and 5*b* calculations for G and ρ_{cold} are presented (at $N = 50$) for the «square-box» distribution. To carry out comparisons, the curve for the single-spark gain is also shown in Fig. 5*a*. The maximum for a single spark ($G_{ss} = 2706$) occurs at $\nu = 0.0483$, and the associated cold fuel density is $\rho = 910$ g/cm^3. This density value is about 0.5 of that associated with the maximum on the curve *5* in Fig. 5*a*. Clearly, substantially more favorable results for multispark follow from the calculations relative to the other distribution functions (see Fig. 1). For the single spark approach, the site of the maximum gain is unlikely to be a working point since it corresponds to spark convergence ratios that are not practical. This can be deduced from prescriptions deriving from some high-gain capsule designs, where at 3/4 of the initial target radius the in-flight aspect ratio (IFAR) is set equal 30 and the total thickness (ablator + DT) is assumed to be equal to that of the initial, solid-state density DT layer [7, 8]. Thus the initial shell radius follows as

$$R_0 = \left(\frac{\text{IFAR}}{3\pi} \frac{M_{fuel}}{\rho_0} \right)^{1/3}, \tag{27}$$

where ρ_0 is the DT density at the solid state. The spark convergence ratio is evaluated as $C_{spark} = R_0/R_{thr}$. The single-spark maximum gain corresponds to $C_{spark} = 99$, a value much greater than those currently accepted [9] (≈ 40). The working value ($C_{spark} = 40$) is recovered at $\nu = 0.308$, where the gain is $G_{ssw} = 1741$. This working point was labelled W in Fig. 5*a*. The gain at W is smaller than the maximum gain obtained with multi-spark systems. For multispark, the geometric parameter corresponding to C_{spark} may be $C_{hot} = R_0/R_s$, where R_s is the radius of the turbulent region (see Sec. 5). For the highest gain $R_s = R_{fuel}$, and $C_{hot} = C_{fuel} = R_0/R_{fuel}$. Under these conditions, the highest gain for the case of Fig. 5*a* corresponds $C_{fuel} = 45$, whereas $C_{fuel} = 39$ for the «power-laws» case. To obtain a gain G_{ssw} by multispark configurations, more relaxed conditions are sufficient, namely those corresponding to $C_{fuel} \approx 38$ for the case of Fig. 5*a*, and $C_{fuel} \approx 30$ for a «power-laws» distribution. These conditions should be used in the implosion design, taking into account that in a multispark assembly the overall shape of the final fuel is expected to play a secondary role in determining thermonuclear performances of the system.

7. CONCLUSIONS

In the conventional ICF approach a central issue is the formation of a spherical triggering spark at the center of the fuel, at the end of the implosion process. Highly deformed sparks do not ignite [1] and in experiments it has been found a substantial deviation of the measured number of neutrons from that computed in $1D$ simulations. This deviation increases with the implosion convergence ratio. The usual interpretation attributes these results to a mixing process.

In this paper we assumed that as a final result of the implosion a multispark system has been generated. It was found that high thermonuclear fuel gain can be still obtained from compressed fuel assemblies, in which a large number of sparks (N = 10–100) with a statistically generated energy (size) spectrum is created. By requiring to have, with an assigned probability, at least one spark large enough to ignite the fuel, we have computed the assembly dimensioning and, by using statistical arguments, the burn fraction and the fuel gain. It was found that the results may depend on the values of two integral parameters, which depend on the energy-space distribution function of the sparks.

Although requiring more compressed fuels (typically $2\times$–$3\times$), the multispark approach may prove to be interesting because (in principle) it is based on the hypothesis of ab initio relaxed implosion symmetry requirements. Final mixing processes, which are currently considered to be adverse in ICF, could turn out to be not so dangerous, since high gain can still be obtained. Based on these considerations, the domain of implosion designs can be expanded so as to make it relevant for thermonuclear energy.

References

1. R. L. McCrory and C. P. Verdon, in *Proc. of the Intern. School Piero Caldirola on Inertial Confinement Fusion*, ed. by A. Caruso and E. Sindoni, Editrice Compositori (1988), p. 83.
2. H. Sakagami and K. Nishihara, Phys. Fluids B **2**, 2715 (1990).
3. H. Sakagami and K. Nishihara, Phys. Rev. Lett. **42**, 432 (1990).
4. S. Yu. Gus'kov, O. N. Krokhin, and V. B. Rozanov, Nucl. Fusion **16**, 957 (1976).
5. M. D. Rosen, J. D. Lindl, and A. R. Thiessen, LLNL Annual Report (1983).
6. L. D. Landau and E. M. Lifshitz, *Theoretical Physics, Vol. 5*, Pergamon Press (1980), pp. 162–166.
7. A. Caruso, in *Proc. of the Intern. School Piero Caldirola on Inertial Confinement Fusion*, ed. by A. Caruso and E. Sindoni, Editrice Compositori (1988), p. 139.
8. J. Lindl, Phys. Plasmas **2**, 3933 (1995).
9. J. Lindl, in *Proc. of the Intern. School Piero Caldirola on Inertial Confinement Fusion*, ed. by A. Caruso and E. Sindoni, Editrice Compositori (1988), p. 595.